MOLECULAR AND CELLULAR BIOLOGY, Jan. 2000, p. 249–260 Vol. 20, No. 1
0270-7306/99/$04.00+0

The Rous Sarcoma Virus Env Glycoprotein Contains a Highly Conserved Motif Homologous to Tyrosine-Based Endocytosis Signals and Displays an Unusual Internalization Phenotype

CHRISTINA OCHSENBAUER, SUSAN R. DUBAY, AND ERIC HUNTER*

Department of Microbiology, University of Alabama at Birmingham, Birmingham, Alabama 35294

Received 2 August 1999/Returned for modification 1 September 1999/Accepted 5 October 1999

The cytoplasmic domains of retroviral transmembrane (TM) glycoproteins contain conserved sequence motifs that resemble tyrosine-based (YXXØ-type) endocytosis signals. We have previously described a mutant Rous sarcoma virus (RSV) Env protein, Env-μ26, with an L165R mutation in the membrane-spanning domain (MSD) of TM, that exhibited dramatically decreased steady-state surface expression (G. L. Davis and E. Hunter, J. Cell Biol. 105:1191–1203, 1987; P. B. Johnston, J. Y. Dong, and E. Hunter, Virology 206:353–361, 1995). We now demonstrate that the tyrosine of the Y_{190}RKM motif in the RSV TM cytoplasmic domain is crucial for the μ26 phenotype and is part of an efficient internalization signal in the context of a mutant MSD. In contrast, despite the presence of the Y_{190}RKM motif, wild-type RSV Env is constitutively internalized at a slow rate (1.1%/min) more characteristic of bulk uptake during membrane turnover than of active clustering into endocytic vesicles. The μ26 mutation and two MSD mutations that abrogate palmitoylation of TM resulted in enhanced Env endocytosis indicative of active concentration into coated pits. Surprisingly, an Env-Y190A mutant was apparently excluded from coated pits since its uptake rate of 0.3%/min was significantly below that expected for the bulk rate. We suggest that in RSV Env an inherently functional endocytosis motif is silenced by a counteracting determinant in the MSD that acts to prevent clustering of Env into endocytic vesicles. Mutations in either the cytoplasmic tail or the MSD that inactivate one of the two counteracting signals would thus render the remaining determinant dominant.

Numerous studies have contributed to an increasingly complex picture of the spatial and biochemical organization of the intracellular targeting pathways that include endocytosis (see reference 65 for an overview). Plasma membrane proteins fall into three basic categories regarding their internalization. The first class of glycoproteins undergoes rapid endocytosis via clathrin-coated vesicles, either constitutively, like the low-density lipoprotein (LDL) and the transferrin (Tf) receptors (8), or after activation by ligand binding as for the epidermal growth factor receptor (9, 10). Clustering of proteins into areas of coated-pit formation occurs by interaction of specific amino acid motifs within their cytoplasmic domains with adapter proteins such as AP-2 (4, 5, 42, 43). Two main endocytosis signals have been identified. One contains a critical tyrosine in the context of a YXXØ motif in which Ø represents a bulky, aliphatic residue and for which a consensus sequence can otherwise only be broadly defined. Such a motif can act independently of its position, orientation, and structural context (63) and shows a tendency to form a tight turn (2, 12, 17, 52). YXXØ motifs are present in the Tf receptor (TfR) and the mannose-6-phosphate receptor (12), as well as in TGN38 (20), and the LDL receptor contains a related NPXY motif (11). The second type of endocytosis signal is a dileucine-containing motif, which, like the YXXØ motif, is transferable onto other membrane proteins (23). Constitutive internalization at the rate of membrane bulk uptake (~1 to 2%/min) (64) is characteristic of the second class of plasma membrane glycoproteins. These proteins are believed to enter clathrin-coated pits by default, since no concentration occurs (63). The third class of glycoproteins are endocytosed at a very low rate and are essentially excluded from coated-pit structures. The influenza virus hemagglutinin (HA) protein is by far the best-characterized example of this group, and its exclusion from endocytic vesicles seems to be governed by sequences in its membrane-spanning domain (MSD) (references 32, 35, and 58 and references therein).

Proteins reaching the early-sorting endosome enter either the late endosome/lysosome pathway, ultimately leading to degradation, or the recycling endosome compartment (for a review see reference 41). There is evidence that transport of some proteins into the lysosomal pathway requires a positive signal that is related to either the YXXØ endocytosis signals or a dileucine motif (63). Though these motifs may overlap with internalization signals, they are distinct entities and are crucially defined by their positions in the cytoplasmic tail (28, 54, 65). Lack of such sorting information thus would direct a protein into the recycling pathway by default as suggested by studies of TfR and Lamp-1 (25, 26, 39, 54, 65). In polarized cells, apically endocytosed membrane proteins can also be targeted basolaterally, and for several proteins this process is again governed by tyrosine-containing signals, often found to be colinear or overlapping with YXXØ endocytosis motifs (7, 19, 38). The specificity of the different intracellular targeting pathways, while involving similar or overlapping signal sequences, appears to be achieved by the interaction of the motifs with different adapter protein classes (see reference 60 for an overview).

A comparison of the cytoplasmic C termini of both avian and mammalian retroviral envelope (Env) proteins reveals a remarkable sequence conservation within each group. In particular, the sequences that encompass a motif that is very similar to the YXXØ endocytosis motif consensus sequence are highly conserved in both amino acid composition and distance to the

* Corresponding author. Mailing address: Department of Microbiology, University of Alabama at Birmingham, 845 19th St. South, Birmingham, AL 35294. Phone: (205) 934-4321. Fax: (205) 934-1640. E-mail: ehunter@uab.edu.

MSD (Fig. 1a). Because Env proteins are generally considered to be highly variable, this sequence conservation points to a biologically important role for such motifs in the survival of retroviruses in vivo. Retroviral glycoproteins are crucial for the binding of virions to their cellular receptors, followed by induction of virus-cell membrane fusion and infection. Env proteins are synthesized as precursor molecules that are proteolytically cleaved into the SU (surface) and TM (transmembrane) subunits before delivery to the cell surface, where they are incorporated into budding virions. Both human immunodeficiency virus type 1 (HIV-1) and simian immunodeficiency virus (SIV) glycoproteins have been shown to be efficiently and constitutively internalized from the plasma membrane through coated pits by virtue of their tyrosine motifs (4, 18, 31, 56, 57). Interestingly, coexpression of HIV-1 Gag, the capsid precursor protein, downregulates Env endocytosis (18), possibly by competing for Env interaction with cellular factors such as AP-2. The Env protein of HIV-1 and those of HIV-2 and SIV are targeted to the basolateral surface in polarized cells (1, 45, 46), and HIV-1 Env redirects virion release to this site (37, 46), with the membrane-proximal tyrosine in its cytoplasmic domain being crucial for polarized targeting (38).

The putative endocytosis motif (YXXØ) in the glycoproteins of avian leukosis and sarcoma viruses (ALSV) is remarkably conserved both in sequence and in position within the cytoplasmic domain relative to the transmembranal domain. We have previously described a mutant Prague C strain (PrC) Rous sarcoma virus (RSV) Env protein, Env-μ26, in which a L165R mutation in the MSD of TM dramatically decreased steady-state surface expression of Env with rapid internalization from the plasma membrane and lysosomal degradation (13, 27). From this observation arose the initial questions of whether the tyrosine in the Y_{190}RKM motif found in RSV PrC TM glycoproteins contributes to the very rapid endocytosis observed for Env-μ26 and whether the wild-type glycoprotein displays a phenotype similar to those of other (retro)viral Env proteins. To facilitate a quantitative study of the internalization of RSV PrC Env, we utilized Env proteolytic processing mutant Env-S19 (15, 27). The Env precursor, Pr95, is not cleaved to gp85 (SU) and gp37 (TM) in the trans-Golgi network but is delivered to the cell surface in an uncleaved and fully glycosylated form, gp120. The rate of its biosynthesis, intracellular transport, and incorporation into RSV virions, however, is indistinguishable from that of wild-type Env. Of advantage to us was the unique property that Env-S19 present on the plasma membrane or in virions can be specifically cleaved into gp37 and gp85 by addition of trypsin to the medium, thereby distinguishing surface-exposed from intracellular molecules; mutant Env-S19 treated this way regains its biological function, thus rendering virions infectious (15).

We show here that a wild-type ALSV Env protein has unusual endocytic properties in that the active YRKM endocytosis signal is silenced by sequences in the MSD. Thus, wild-type Env is endocytosed with kinetics similar to those defining the bulk rate turnover of membranes. This low rate of internalization is significantly reduced further by mutation of the critical tyrosine in the YRKM motif. Mutations in the MSD region of the glycoprotein "activate" recognition of the endocytosis signal. To our knowledge there is no precedent for the unusual phenotype of RSV Env, and we discuss a model of the underlying mechanism.

MATERIALS AND METHODS

Expression vectors and RSV Env mutants. In most experiments, wild-type RSV PrC Env and mutants thereof were expressed from recombinant simian virus 40 (SV40) expression vector pSVenvKX, described previously (13). In pSVenvKX-S19, the codons for the proteolytic cleavage site (amino acids [aa] $RRKR_{341}$) of pr95 (to gp85 and gp37) are mutated to code for SRER (15). In pSVenvKX-μ26, the codon for aa L_{165} (in the TM MSD) is changed to code for R (13, 27). In pSVenvKX-palm#6 and -palm#7, aa C_{164} and C_{167}, respectively, are mutated to G (D. C. Miller, C. R. Roberts, S. S. Rhee, and E. Hunter, submitted for publication). Further TM cytoplasmic tail single and double mutants were created in the background of the plasmid pSR-KX by single-strand mutagenesis. In pSR-KX, the *Kpn*I/*Xba*I RSV *env* fragment from pSVenvKX was inserted into pSRHS (16), an expression vector under the control of the SV40 late promoter. The mutations N185*, Y186A, and Y190A were created by mutating nucleotides (nt) 6822 to 6825 (AAC) to TAA, nt 6826 to 6828 (TAT) to GCT, and nt 6837 to 6839 (TAC) to GCC, respectively (nucleotide numbering is according to the RSV pATV-8 sequence [29]). In addition, a μ26/Y190A double mutation was created. pSVenvKX plasmids containing codons for the S19 mutation combined with codons for mutations in TM were cloned as follows. The 1,089-bp *Xho*I/*Sma*I fragment containing S19 from pSR-env-S19 was inserted into pSVenvKX-palm#6, -palm#7, -μ26/Y190A, and -N185*. The 507-bp *Sma*I/*Xba*I fragment from pSR-env-Y190A was inserted into pSVenvKX-S19 to create pSVenvKX-S19/Y190A. The presence of all mutations was verified by dideoxy sequencing. Influenza virus A/Jap/305/57 wild-type HA was expressed from pSVsHA as described previously (14). Plasmids pksSVEHA−Y543 and pksSVEHA+8 were received from Mike Roth and have been described previously (33).

Expression of plasmid vectors and recombinant SV40 in CV-1 cells. African green monkey kidney cells (CV-1) were obtained from the American Type Culture Collection (Manassas, Va.). Cells were maintained in Dulbecco modified Eagle medium (DMEM) supplemented with 10% fetal calf serum (FCS).

Transfections were performed by the calcium phosphate precipitation method. CV-1 cells (2×10^5) were plated on 60-mm-diameter plates 1 day prior to transfection. Cells were washed 18 h posttransfection, and those transfected with pSR-KX plasmids were analyzed 48 h later. To prepare recombinant SV40 virus stocks, as described previously (33), the respective plasmids were first digested with *Kpn*I to remove plasmid sequences and self-ligated to juxtapose the SV40 late promoter with the 5′ end of the *env* or *HA* gene. DNAs were cotransfected with *dl*1055 helper virus DNA (51).

At 5 days posttransfection, Env and HA expression was analyzed by immunofluorescence, and cells were lysed by repeated freezing and thawing and sonication. Undiluted lysate was used to infect fresh CV-1 cells. High-titer lysates from a second round of infection were stored frozen. Four hundred microliters of working dilutions of 1:5 to 1:8 were used to infect CV-1 cells, plated at 2×10^5 the day before onto 60-mm-diameter plates. Experiments were performed 42 to 48 h postinfection, when cells showed only a moderate cytopathic effect but already a high level of Env expression.

Antisera used. Polyclonal rb#2 anti-gp85 antibody specifically interacts with RSV SU (gp85) protein. Anti-RSV-TMpep, which was raised against a C-terminal peptide (Cys plus aa 184 to 198) of RSV PrC TM, was a gift from Judy White. Chicken anti-RSV PrC neutralizing antibody has been described previously (27). rb_{wonton} anti-HA_{Jap} is specific for influenza virus A/Jap/305/57 HA and was received from Mary-Jane Gething.

Metabolic labeling and cell surface biotinylation. CV-1 cells expressing wild-type and mutant Env or HA were labeled with 200 μCi of EXPRE^{35}S [^{35}S]methionine-cysteine labeling mixture (NEN, Boston, Mass.) in 400 μl of methionine-deficient medium or phosphate-buffered saline (PBS). After a 30-min pulse at 37°C, cells were lysed either immediately or after a 2-h chase in complete medium. Where appropriate, 60-mm-diameter plates of cells were washed four times in PBS-MC (1 mM $MgCl_2$, 0.1 mM $CaCl_2$) and cell surface proteins were biotinylated with 1.5 ml of EZLink-Sulfo-NHS-LC-Biotin (Pierce; 0.5 mg per ml of PBS-MC) on ice at 4°C for 30 min. Nonbound biotin was then quenched with 20 mM glycine in DMEM for 10 min on ice before cells were washed in cold PBS and either lysed or subjected to an internalization or raft association assay. Cells lysed directly after biotinylation were subjected to Env immunoprecipitation followed by enhanced chemiluminescence Western blot analysis with horseradish peroxidase-coupled streptavidin.

Internalization of surface-biotinylated proteins. Assays to determine the rate of internalization of wild-type RSV Env and mutants were performed with the Env-S19 cleavage mutant. As has been shown previously (15), Env-S19 expressed on the cell surface (as fully glycosylated precursor gp120) can be specifically cleaved into gp85 and gp37 by the addition of trypsin to the medium with the retention of biological Env function. After surface biotinylation on ice, cells were warmed to 37°C by the addition of warm DMEM-FCS in the absence or presence of chloroquine (100 μM) and maintained at 37°C for various times (0 to 90 min). Samples were then washed three times with PBS on ice and incubated with 5 μg of tolylsulfonyl phenylalanyl chloromethyl ketone (TPCK)-trypsin per ml of DMEM (FCS free; adjusted to pH 9) at 4°C for 50 min. Soybean trypsin inhibitor at 200 μg/ml was then added for 5 min. We observed that trypsin treatment could result in detachment of a portion of the cells, especially those that after biotinylation on ice were not returned to 37°C, which seemed to increase attachment. Therefore, all plates were carefully washed in PBS to remove detached and potentially damaged cells before samples were lysed in buffer containing 1% Triton X-100 and 1% deoxycholate (DOC). After the nuclei were spun down, cell lysates were adjusted to a sodium dodecyl sulfate (SDS) concentration of 0.1% and subjected to Env or HA immunoprecipitations. Precipitates were washed

and released from protein A by being boiled for 5 min in 20 μl of 5% SDS. Six hundred microliters of SDS-free lysis buffer was added to the supernatants, and biotinylated proteins were recovered by the addition of streptavidin beads (Pierce) overnight at 4°C. Washed precipitates were then boiled for 10 min in 12% SDS prior to SDS-polyacrylamide gel electrophoresis (PAGE), autoradiography, and quantitation by PhosphorImager (Molecular Dynamics) analysis.

Calculating the relative amounts of internalized, biotinylated Env. PhosphorImager scans were analyzed with the program ImageQuant (Molecular Dynamics). For Env internalization analysis, gp120, gp85, and gp37 bands, for all time points of 37°C chases that were followed by trypsin treatment, were quantified and corrected for background in each lane.

We made the assumption that at all time points the same relative amount of labeled, biotinylated surface-residual gp120 remains inaccessible for cleavage. This allowed us to correct for incomplete cleavage by using the following relationships. The relative amount of apparently cleavage-protected Env at time t_n (AP_n) is composed of the portion of actually endocytosed Env (E_n) and surface-residual Env remaining uncleaved (U_n): $AP_n = E_n + U_n$. The fraction of Env on the surface (S_n) is composed of the fraction of cleaved Env (C_n) and U_n: $S_n = C_n + U_n$. Only AP_n and C_n are directly measurable, with $AP_n + C_n = 1$. The value of interest is the portion of endocytosed Env at times t_n, E_n, which can be derived from measured values based on the following relationships. At $t_{n=0}$, E_0 is zero and thus $AP_0 = U_0$. U_0, the portion of surface-residual Env remaining uncleaved, can also be expressed as a fraction (X_0) of S_0: $U_0 = X_0 \cdot S_0$ or $X_0 = U_0/S_0$ or $X_0 = U_0/(C_0 + U_0)$ or $X_0 = AP_0/(C_0 + AP_0)$, since $E_0 = 0$. Since we assume that at all time points the same relative amount of surface-residual gp120 remains inaccessible for cleavage, we can use the equation $X_0 = AP_0/(AP_0 + C_0)$ to correct for that at $t_{n>0}$. After a series of mathematical operations it finally follows that $E_n = 1 - (C_n/1 - X_0)$. From the scan data we determined X_0 and all C_n and thus obtained the relative amount of truly internalized Env at each time point.

Statistical determination of endocytosis rates. Uptake rates for the wild-type and mutant Env-S19 proteins were calculated as follows. For each Env protein, the data from independent experiments were plotted, and the individual uptake rates were computed by linear regression analyses of the initial 10-min chase period. Then, the mean endocytosis rates (X_n) and standard deviations (S_n) were calculated for all Env constructs. The resulting rate for each of the Env-S19 mutants was compared with that for the wild type in a two-sample, one-sided Student t test with $\alpha = 0.01$ under the assumption that the population variances (μ_n), though unknown, are equal: $t = [(x_1 - x_2) - (\mu_1 - \mu_2)]/[(S_p^2/n_1) + (S_p^2/n_2)]^{1/2}$ where $S_p^2 = [(n_1 - 1)S_1^2 + (n_2 - 1)S_2^2]/(n_1 + n_2 - 2)$. For the purpose of graphic presentation a simplified approach was chosen: for all respective Env proteins at each time point the mean values and standard deviations of the relative amounts of endocytosed Env were determined and plotted.

DIG association assay. Wild-type and mutant RSV Env proteins were tested for their potential presence in cholesterol- and glycolipid-rich plasma membrane domains called rafts or detergent-insoluble glycolipids (DIGs) by following a protocol described previously (58). Essentially, Env- and HA-expressing cells were metabolically labeled and biotinylated as described above. Samples were then washed on ice, taken to the 4°C room, and lysed on ice for 5 min in TNE (50 mM Tris-HCl [pH 7.5], 150 mM NaCl, 2 mM EDTA, 2 mM dithiothreitol, 1× proteinase inhibitor cocktail [Boehringer GmbH, Mannheim, Germany]). Lysates were transferred to precooled tubes, spun at 12,000 × *g* for 6 min at 4°C, and returned to ice. Supernatants containing the detergent-soluble membrane fraction were separated from pellet material insoluble in Triton X-100 under the given temperature conditions. Supernatants were adjusted to achieve an SDS concentration of 0.1%; pellets were dissolved in lysis buffer containing 1% Triton X-100, 1% DOC, and 0.1% SDS. Samples were then subjected to immunoprecipitation followed by retrieval of biotinylated proteins as described above and SDS-PAGE analysis.

Indirect immunofluorescence analysis. To test for transfection and infection efficiencies and steady-state intracellular Env and HA distribution, protein-expressing CV-1 cells grown on glass coverslips were fixed in cold acetone and then probed with either rabbit (rb) anti-Env (rb#2) or anti-HA (rb_{wonton}) serum, with goat (gt) anti-rb–fluorescein isothiocyanate (FITC) as the second antibody. For surface immunofluorescence, unfixed cells on coverslips were incubated with the respective first antibody on ice for 30 min, washed, fixed with methanol-acetic acid, and stained with gt anti-rb–FITC. In order to compare levels of internalization of wild-type and mutant Env, CV-1 cells grown on coverslips were washed in PBS at 42 to 48 h postinfection. Cells were then incubated with 100 μl of DMEM containing chicken anti-RSV PrC neutralizing serum (diluted 1:20) and 100 μM chloroquine (to prevent lysosomal degradation of endocytosed Env and antibodies) at 37°C for 2 h. Thereafter, cells were washed in PBS, fixed with methanol-acetic acid, and stained with rb anti-chicken–FITC. All samples were observed with a Zeiss fluorescence microscope.

RESULTS

Cell surface expression of the rapidly endocytosed RSV Env mutant Env-μ26 (L165R) can be restored by additionally removing a crucial tyrosine in the cytoplasmic domain. To determine whether tyrosine (Y_{190}) present in the cytoplasmic domain of RSV TM contributes to the rapid internalization of Env-μ26 (L165R) from the cell surface, we analyzed the biosynthesis and steady-state surface expression of several mutants. We first engineered mutations in the cytoplasmic tail of RSV PrC TM, removing one or both of the two potentially important tyrosines (mutations Y190A, Y186A, and $N185^{*stop}$). While Y_{190} is found in the sequence context of a YXXØ motif (YRKM), this is not the case for Y_{186} (YHTE). The positions and designations of mutants used throughout this study are shown in Fig. 1b. Wild-type Env, Env-μ26, Env-Y190A, and Env-μ26/Y190A were expressed in CV-1 cells after transfection with pSR-env vectors (see Materials and Methods). Metabolic labeling of these mutants (Fig. 2a), as well as of Env-Y186A, Env-μ26/Y186A, Env-N185*, and Env-μ26/N185* (not shown), revealed that all Env proteins were synthesized and posttranslationally modified (i.e., glycosylated and proteolytically cleaved) at comparable rates during a 30-min pulse and 1-h chase. Env, surface expressed at steady state, was visualized following surface biotinylation (Fig. 2b). As had been observed previously, Env-μ26 surface expression was dramatically reduced compared to that of the wild type (27). In contrast, the amount of the tyrosine-to-alanine mutant glycoprotein, Env-Y190A, that accumulated on the surface was found to be not dramatically different from that of the wild type in repeated experiments, although more-intense gp37 bands were consistently observed for these mutants in this nonquantitative approach. This was also true for Env-Y186A and the truncation mutant Env-N185* (data not shown). The Env-μ26/Y190A double mutant showed a reversion of the μ26 phenotype since surface expression was restored to a level similar to that of the wild type (Fig. 2b). The tyrosine-to-alanine mutation in Env-μ26/Y186A, in contrast, had only a minor effect (data not shown). Since additionally the sequence context of Y_{186} does not corroborate a potential role in endocytosis, Env-μ26/Y186A was omitted from kinetic analyses. Env-μ26/N185* (not shown) had a steady-state distribution phenotype essentially indistinguishable from that of the wild type and Env-μ26/Y190A. From these initial results we concluded that Y_{190} can act as part of an endocytosis motif in the context of the μ26 mutation, since its removal results in the loss of rapid Env-μ26 internalization.

Since wild-type RSV Env displayed a much higher surface expression than Env-μ26, we investigated whether the YRKM motif acted as an endocytosis signal in the context of the wild-type MSD or was silent in this context.

RSV PrC Env is endocytosed from the cell surface with a rate similar to that of bulk membrane uptake despite the presence of a putative tyrosine-based endocytosis motif. Our experimental approach to measure the uptake of Env plasma membrane proteins into intracellular compartments took advantage of RSV Env proteolytic cleavage site mutant S19 (15, 27), mentioned above. In this mutant, the Env precursor, Pr95, is not cleaved to gp85 and gp37 in the trans-Golgi network but is delivered to the cell surface in an uncleaved and fully glycosylated form, gp120. Env-S19 present on the plasma membrane or in virions, however, can be specifically cleaved into gp37 and gp85 by the addition of 5 μg of TPCK-trypsin/ml to the medium (15). Env glycoproteins on the cell surface at $t = 0$ were biotinylated on ice in the first labeling step. Then, after incubating Env-S19-expressing cells at 37°C for various times to allow endocytosis to occur, residual surface gp120 was distinguished from endocytosed molecules by trypsin cleavage at 4°C (see Materials and Methods).

CV-1 cells were infected with recombinant SV40 virus stocks (13) for a reproducibly high level of expression of the glycoprotein of interest. Figure 3a depicts a typical result of an

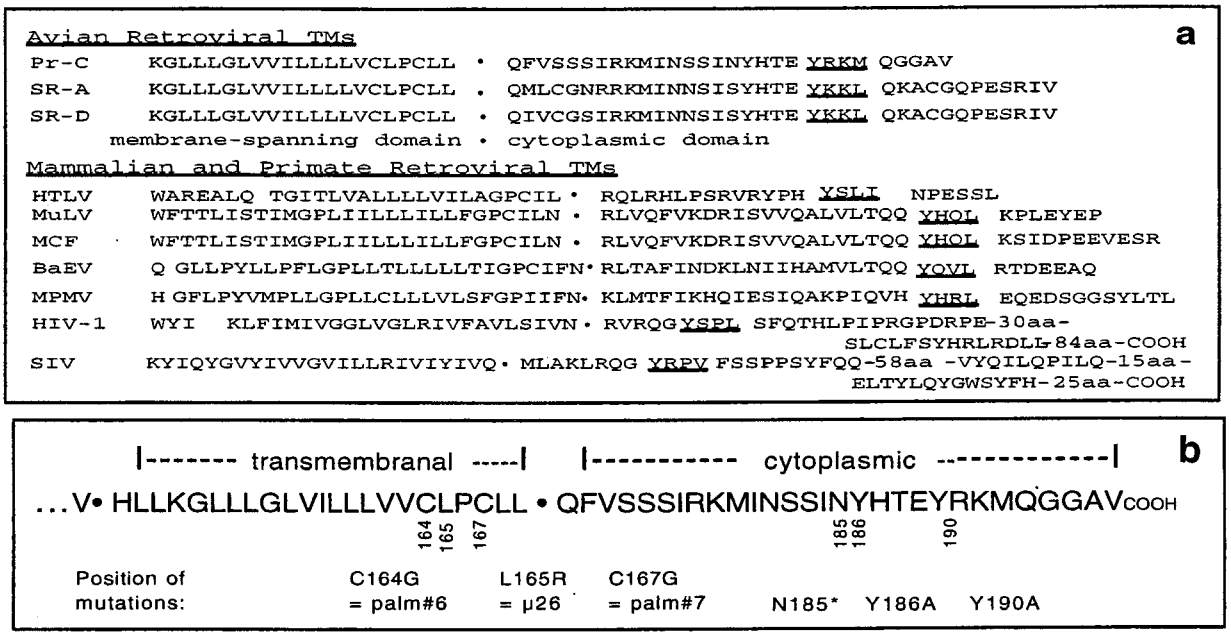

FIG. 1. Conserved amino acid motifs in the cytoplasmic domains of retroviral TM proteins are homologous to tyrosine-based intracellular targeting signals. (a) Sequences of the MSD and cytoplasmic domains and the putative boundaries between them for avian and mammalian retroviral TM proteins. Motifs containing the highly conserved tyrosines (Y) are underlined. SR-A and -D, Schmidt-Ruppin A and D, respectively, RSV strains; HTLV, human T-cell leukemia virus; MuLV, murine leukemia virus; MCF, mink cell focus-forming virus; BaEV, baboon endogenous virus; MPMV, Mason-Pfizer monkey virus. (b) Sequences of the RSV PrC TM protein MSD and cytoplasmic domain. The boundaries of the MSD as shown here were derived from previous studies (Miller et al., submitted); C_{164} and C_{167} have been shown to be palmitylated (Miller et al., submitted) and to be embedded in the lipid bilayer. The positions and designations of RSV PrC mutants used in this study are indicated.

Env-S19 internalization assay, in which 100 μM chloroquine was added to the chase medium to prevent potential lysosomal degradation of internalized protein. Samples not treated with trypsin show the expected gp120 band. Trypsin treatment without a prior 37°C chase resulted in a 96 ± 3% efficiency of cleavage into gp37 and gp85. With increasing chase duration, the protection of gp120 from cleavage, due to internalization, becomes apparent. When the proportion of Env endocytosed at each time point was calculated as described in Materials and Methods and plotted (Fig. 3b), the curve of Env precursor protection from proteolysis is biphasic. In the first 10 to 15 min, internalization is likely the only process contributing to the data, and it can be assumed that the flattening of the curve at later time points is due to the onset of Env recycling to the surface (see reference 32 on the kinetics of recycling in CV-1 cells). The average endocytosis rate of Env-S19 was thus calculated for the linear phase of the uptake kinetics (see Materials and Methods) and was determined to be 1.1%/min. Chloroquine has been described as inhibiting lysosomal protein delivery and degradation but also as adversely affecting trafficking routes of ligand-binding receptors when present for an extended time period. However, it is not likely to affect endocytosis rates early after its addition (36), and the validity of this assumption in our assay is confirmed by Fig. 4. Furthermore, recycling of a membrane protein that, like Env, does not require release of a ligand was found to be undisturbed by weak lysosomotropic bases (36). To corroborate the validity of our observation, we expressed influenza virus HA mutant HA-Y543 (obtained from M. Roth) in parallel experiments (data not shown). This HA mutant was reported to exhibit an initial internalization rate of ~4%/min in CV-1 cells (30, 34), and we observed an equivalent rate in the experiments performed here.

Since the rates of bulk membrane and protein uptake in CV-1 cells and other cell types have been described to be 1 to 2% per min (32, 47), it was somewhat surprising that RSV Env, which contains a YXXØ endocytosis motif consensus sequence, showed an uptake rate equal to or slightly lower than that reported for the bulk membrane uptake. Internalization of proteins at the rate of membrane turnover does not require any specific uptake signals since no active concentration into coated pits occurs (for a review, see reference 63). However, the internalization rates of certain endocytosis motif-containing receptors can be activated to significantly higher levels. For example, the chemokine receptor CXCR4 shows constitutive bulk uptake (1%/min) that can be enhanced by ligand binding (59).

In order to investigate whether the binding of neutralizing antibodies to plasma membrane-associated Env could enhance endocytosis, possibly by inducing conformational changes in the external domains or by capping the protein on the membrane, the experiments described above were repeated in the presence of neutralizing antibodies. There was no evidence for enhancement when surface-biotinylated CV-1 cells expressing Env-S19 were preincubated with chicken anti-RSV PrC serum prior to shifting them back to 37°C for the indicated times (Fig. 3c).

A fraction of RSV PrC Env is intracellularly degraded after internalization in the absence of chloroquine. We were interested in determining if part of the internalized wild-type Env protein was targeted for lysosomal degradation, a process that takes place rapidly and efficiently with Env-μ26 (27). The experiments were performed essentially as described for Fig. 3, but duplicate samples were analyzed, with chloroquine (100 μM) being either included or omitted in the 37°C chase medium (Fig. 4). Chasing in the presence of chloroquine resulted in the previously observed biphasic curve, whereas when chloroquine was omitted during the chase, the portion of detectable Env that was uncleaved decreased over time after reaching a maximum at ~30 min, due to lysosomal degradation.

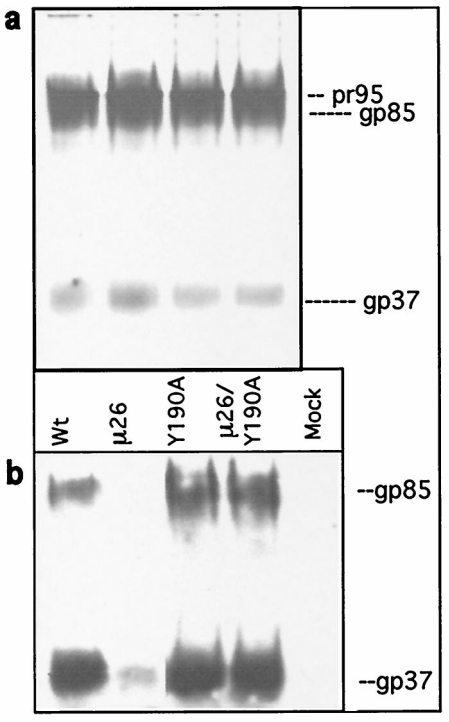

FIG. 2. The highly reduced steady-state surface expression of Env mutant Env-μ26 can be restored to approximately wild-type levels by removing Y_{190}. (a) CV-1 cells were transfected with pSR-Env plasmid vectors encoding the indicated wild-type (wt) and mutant Env proteins. After metabolic pulse-labeling with [^{35}S]methionine-cysteine for 30 min and chasing for 1 h in complete DMEM, cells were washed, lysed, and subjected to rb#2 anti-Env immunoprecipitations and analyzed by SDS-PAGE and autoradiography. Unglycosylated (pr95) Env precursors, as well as the mature cleavage products gp37 (TM) and gp85 (SU), were detected. (b) A second set of transfected cells was surface biotinylated for 30 min on ice and then lysed and subjected to rb#2 anti-Env immunoprecipitation followed by SDS-PAGE and enhanced chemiluminescence Western blotting. Streptavidin was then used to visualize steady-state levels of Env surface expression.

However, internalization kinetics within the first 10 to 15 min were equal in both cases. Without withdrawal of Env into the lysosomal compartment, internalization and recycling would be expected to establish a steady-state Env distribution internally and on the surface, and one might expect to see a plateau value for intracellular cleavage-protected Env. In contrast, the biphasic curve observed when chloroquine was included in the 37°C chase medium shows an accumulation of protease-protected Env and thus would argue for a fraction of the molecules being withdrawn from recycling. The degradation of gp120 observed in the absence of chloroquine is consistent with this interpretation, since in this case these nonrecycling molecules would be rapidly degraded in the lysosome.

Mutations in the RSV TM transmembranal domain increase the rate of endocytosis, while exchange of Y_{190} for A significantly reduces the endocytosis rate. The results presented in Fig. 2b provided information only about the steady-state surface distribution of different Env mutants, with endocytosis, recycling, and degradation each contributing to the equilibrium state. We were therefore interested in quantitatively determining, for various Env mutants, the effect of the amino acid changes on internalization rates. In addition to the cytoplasmic tail mutation Y190A and the MSD mutation μ26, further mutations in the MSD, C164G (palm#6) and C167G (palm#7), were analyzed. Mutations palm#6 and palm#7 specifically abrogate palmitoylation at C_{164} and C_{167}, respectively, and result in decreased steady-state cell surface expression of monopalmitoylated Env and enhanced intracellular degradation (Miller et al., submitted). The μ26 (L165R) mutation, though adjacent to the respective sites, does not affect palmitoylation (13). Though C167G (palm#7) shows more pronounced effects than C164G (palm#6), they are less dramatic than those of μ26 (L165R). RSV virions carrying any of these three MSD mutations, which might induce conformational changes in the MSD of Env, exhibited impairment or loss of infectivity in turkey cells (13; Miller et al., submitted)). Internalization assays were performed in the presence of chloroquine, essentially as described above. A typical experiment included Env-S19 with a wild-type MSD and cytoplasmic tail (wild-type Env-S19), Env-S19-palm#6, Env-S19-palm#7, and Env-S19-Y190A. Even with only the limited number of post-biotinylation incubation times (0, 10, or 30 min at 37°C) shown in Fig. 5a, it is apparent that the Env precursor of Env-S19-palm#7 is more rapidly and more extensively protected from trypsin cleavage than are the wild-type Env-S19 and Env-S19-palm#6 proteins. In contrast, the Env-S19-Y190A mutant shows a surprisingly slower onset of cleavage protection and thus internalization. The quantitative data from three to five experiments per time point, for each of the above mutants and Env-S19-μ26, were averaged and plotted (Fig. 5b). Average endocytosis rates as revealed by regression analyses of the linear parts of the curves (the initial 10 min of a chase) are shown in Table 1. Internalization of Env-S19-μ26 and Env-S19-palm#7 is very fast and consistent with the concentration of the mutant Env in clathrin-coated pits and active endocytosis (63). The kinetics of Env-S19-palm#6 internalization, however, are still in accordance with passive membrane bulk uptake and are not significantly different from those of the wild type ($P > 0.1$). Unexpectedly, the endocytosis rate exhibited by Env-S19/Y190A (0.3%/min) is significantly lower ($P \leq 0.005$) than that of the wild type. This very slow rate is similar to that of influenza virus HA (0.2%/min in CV-1 cells [32]), a protein shown to be actively excluded from clathrin-coated pits (6, 33, 55). To our knowledge this is the first study in which substitution of a tyrosine within a known YXXØ endocytosis motif resulted in a decrease in the uptake rate to below that of bulk uptake.

The results of the cleavage protection experiments were confirmed by immunofluorescence analyses of the uptake of surface-bound neutralizing chicken anti-PrC antibody (Fig. 6). In the presence of chloroquine, Env proteins with mutations in the MSD showed an increasing accumulation of endocytic vesicles which contained chicken anti-PrC antibody lining the inner vesicle surface and that could be brightly stained with rb anti-chicken-FITC antibodies after fixation. The vesicles observed tended to cluster near the nucleus and can be considered prelysosomal (27, 36, 53). The increasing accumulation of antibody in intracytoplasmic vesicles (wild type < Env-S19-palm#6 < Env-S19-palm#7 < Env-S19-μ26) paralleled the differences in uptake rates determined from the proteolysis protection experiments. At the same time, staining of the cell boundaries decreased accordingly for each of these mutants (Fig. 6). In contrast, Env-S19-Y190A and Env-S19-N185* showed extensive plasma membrane staining and very few fluorescent endocytic vesicles, consistent with very slow uptake of the surface Env. The intensity of staining of Env expressed on the surfaces of unfixed cells on ice (not shown) reflected the equilibrium Env distribution shown in Fig. 2b.

In the Env-S19-μ26/Y190A mutant, two opposing internalization phenotypes partly compensate for each other, resulting in an endocytosis rate similar to that of the wild type. In order to gain insight into the mechanism by which the μ26 mutation increased the rate of endocytosis and to determine the extent

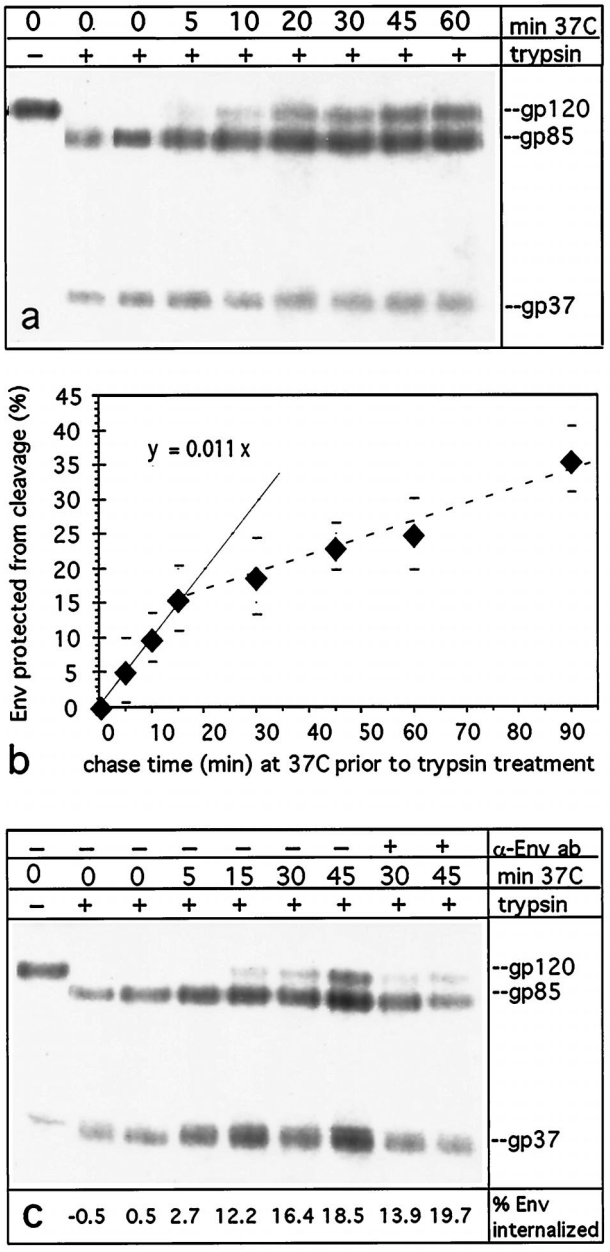

FIG. 3. RSV Env-S19 is internalized and protected from trypsin cleavage during chases at 37°C. CV-1 cells infected with recombinant SV40 virus coding for trypsin-cleavable Env-S19 with a wild-type MSD and cytoplasmic tail were metabolically labeled with [^{35}S]methionine-cysteine (30-min pulse and 2-h chase). Cells were surface biotinylated on ice and then returned to 37°C for the indicated times from 0 to 60 min in complete DMEM (including 100 μM chloroquine to inhibit lysosomal degradation) to allow for endocytosis to occur. Thereafter, surface residual Env-S19 gp120 was cleaved to gp37 and gp85 with 5 μg of TPCK-trypsin/ml at 4°C for 50 min. Cell lysates were consecutively subjected to immunoprecipitation with rb anti-RSV-TMpep and streptavidin-agarose bead precipitation. Samples were analyzed by SDS-PAGE and autoradiography, and gp120, gp37, and gp85 bands were quantitated with a PhosphorImager (Molecular Dynamics). (a) Autoradiogram of Env-S19 after different lengths of 37°C chases and trypsin treatment; amounts of samples loaded per lane were adjusted to approximately equal cell numbers (see Materials and Methods). Note the increase of internalized, and thus cleavage-protected, gp120 over time. (b) Average uptake of Env expressed as the percentage of cleavage-protected gp120 over time from four to six experiments per data point; error bars are shown. Values were calculated as described in Materials and Methods. The linear regression for the linear part of the curve (first 10 to 15 min) (solid line) reveals an average endocytosis rate of ~1.1%/min. (c) Prebinding of neutralizing chicken anti-PrC antibody (α-Env ab) has no enhancing effect on endocytosis. Cells were prepared as described above, but two samples were incubated with chicken anti-PrC serum (1:100) in DMEM at 4°C for 40 min prior to chasing at 37°C for 30 and 45 min.

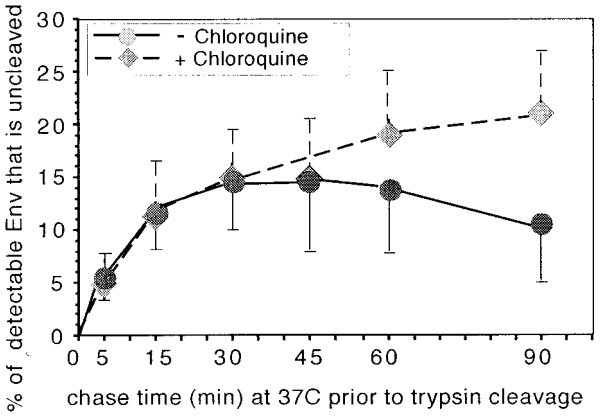

FIG. 4. RSV Env-S19 endocytosis in the presence and absence of chloroquine. Duplicate plates of CV-1 cells were infected, labeled, and biotinylated as described for Fig. 3a. Cells were then chased at 37°C for the indicated times, either in the absence or presence of chloroquine (100 μM). Trypsin treatment and all analyses were done as described for Fig. 3. Average values from three to five experiments per time point are shown.

to which the Y190A mutation can restore the μ26 phenotype to a more wild-type-like phenotype, we cloned the coding sequence for the double mutant (Env-S19-μ26/Y190A) into pSVenvKX-S19 and examined it in the proteolysis protection assay (Fig. 7). Env-S19-μ26/Y190A consistently exhibited a slightly faster uptake than Env-S19 (17.2 versus 11.7% within the first 10 min) (Table 1). It therefore appears that the opposing phenotypes of μ26 (very rapid uptake) and Y190A (very slow uptake) partly compensate for each other.

The internalization phenotypes of wild-type Env and transmembranal and cytoplasmic domain mutants cannot be linked to their differential association with DIG membrane rafts. Recent studies of HA MSD mutants have pointed to a possible correlation between the exclusion of HA from clathrin-coated vesicles and its association with certain plasma membrane domains (DIGs). Both processes appear to be governed by amino acids in the MSD. We therefore investigated whether the dramatically different phenotypes exhibited by the MSD and cytoplasmic domain mutants of RSV Env correlated with partitioning to discrete membrane domains.

The DIG association assay performed is based on the observation that cholesterol- and glycolipid-rich membrane domains (DIGs), and the membrane proteins associated with them, are not soluble in 1% Triton X-100 at 4°C and can be pelleted from cell lysates (see reference 58 for an overview). Proteins recovered from the soluble supernatant are considered to be absent from DIGs. Wild-type Env-S19, Env-S19-μ26, Env-S19-palm#7, and Env-S19-Y190A, as well as wild-type HA as a control (14), were tested for DIG association (Fig. 8). The majority of HA is found in the pellet fraction, as was to be expected (40, 58). In contrast, we did not recover any of the Env proteins tested from the detergent-insoluble fraction. We thus conclude that differential DIG association is not likely to be the basis for the RSV Env mutant endocytosis phenotypes.

DISCUSSION

We have studied the internalization of wild-type and mutant RSV PrC Env glycoproteins to gain insight into the role of a conserved putative endocytosis motif (YXXØ) encompassing amino acids Y_{190}RKM in the cytoplasmic domain of the RSV PrC TM protein. We demonstrate here that a RSV PrC enve-

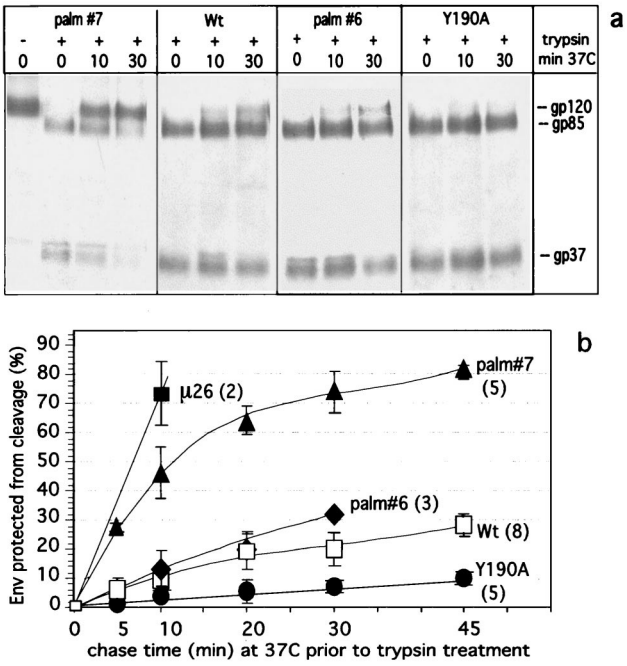

FIG. 5. Mutations in the RSV TM transmembranal and cytoplasmic domains can modulate the endocytosis rate. CV-1 cells were infected with recombinant SV40 lysates expressing Env-S19, Env-S19-Y190A, Env-S19-palm#6, Env-S19-palm#7, and Env-S19/μ26, so that similar expression levels were reached at 2 days postinfection. Cells were then metabolically labeled, chased, and biotinylated on ice as described in Materials and Methods. Replicate plates of cells were chased for different times (0 to 45 min) at 37°C in DMEM–100 μM chloroquine, before surface residual Env gp120 was cleaved into gp85 and gp37 by 5 μg of TPCK-trypsin/ml at 4°C. Cell lysates were subjected to immunoprecipitation and streptavidin-agarose bead precipitation and analyzed by SDS-PAGE, autoradiography, and PhosphorImager quantitation. (a) Autoradiogram of a representative experiment depicting internalization and protection from cleavage of Env-S19 (wild type [wt]) Env-S19-palm#6, Env-S19-palm#7, and Env-S19-Y190A over time. (b) Kinetics of protection from trypsin cleavage of Env-S19 MSD and cytoplasmic mutants compared to wild-type Env-S19 in the presence of chloroquine. Numbers of performed experiments per Env protein are in parentheses. For graphic presentation purposes, mean values and standard deviations at each time point for all Env proteins were determined and plotted.

TABLE 1. Comparison of average endocytosis rates of RSV Env-S19 mutants

Mutation	Avg endocytosis rate[a] (% uptake/min)	No. of expts	Confidence level (P)[b] for:	
			μ (wt) > μ (mutant)	μ (wt) < μ (mutant)
Y190A	0.3 ± 0.2	5	≤0.005	n.a.[e]
None (wild type)	1.1 ± 0.2	8		
palm#6 (C164G)	1.3 ± 0.7	3	n.a.	>0.1
palm#7 (C167G)	4.7 ± 0.9	5	n.a.	≤0.005
μ26 (L165R)	7.4[d]	2[c]	n.a.	≤0.005
μ26/Y190A	1.7 = 0.4[d]	4	n.a.	≤0.01

[a] Rates were derived as follows. For each Env construct, the data of independent experiments were plotted over time, and regression analyses of the linear part (i.e., the initial 10 min) of each curve were performed to obtain the rate constants. Mean values and standard deviations were then calculated for each Env protein.

[b] Confidence level in a two-sample, one-sided t test (see Materials and Methods). Wild-type (wt) and palm#6 uptake rates are not considered significantly different ($P > 0.1$).

[c] Very low Env-μ26 surface biotinylation (14) greatly hinders more-extensive kinetic analyses; range of values ($X_{max} - X_{min}$) for μ26 is 2.6.

[d] No samples were taken between 0 and 10 min; thus a more statistically adequate presentation is 74% within 10 min (μ26) and 17% within 10 min (μ26/Y190A).

[e] n.a., not applicable.

lope glycoprotein with a wild-type TM is indeed endocytosed from the surfaces of CV-1 cells, but at a slow rate (1.1%/min) reminiscent of that of membrane bulk uptake (22, 32, 47) despite the presence of the YRKM motif. In contrast, a quantitative analysis of previously described MSD mutants Env-μ26 (L165R) and Env-palm#7 (C167G) that exhibit significantly reduced steady-state surface expression (27) revealed a much more rapid rate of endocytosis, with an average of 74 and 47%, respectively, being internalized within the initial 10 min of a chase. Tyrosine (Y_{190}) was identified as crucial for the efficient recognition of Env by the internalization machinery in the context of the transmembranal domain mutant Env-S19-μ26, since only about 17% of the Env-S19-μ26/Y190A double mutant was endocytosed within the same time period. Interestingly, uptake of the Env-S19-μ26/Y190A double mutant was similar to, but nevertheless significantly faster than ($P \leq 0.01$), that of wild-type Env. Most surprising was the observation that the Y190A mutation by itself resulted in a further drop of the internalization rate to 0.3%/min, significantly lower ($P \leq 0.005$) than that of the wild type. This indicates active exclusion of the glycoprotein from coated pits and, together with results obtained for the MSD mutants Env-S19-μ26 and Env-S19-palm#7, suggests unique features of the RSV TM internalization motif. The slow internalization exhibited by the YXXØ motif-containing RSV Env protein was unexpected since constitutive endocytosis, clearly faster than bulk membrane uptake, had previously been demonstrated for the lentiviral HIV-1 and SIV Env glycoproteins, for chimeric CD4 molecules carrying the SIV Env cytoplasmic tail (18, 31, 56, 57), and for the varicella-zoster virus (VZV) gE glycoprotein, which contains a conserved YXXØ motif (44).

Uptake kinetics of wild-type Env indicated recycling of internalized viral glycoproteins to the cell surface, while some portion is sorted into the lysosomal pathway. So far, we cannot rule out the possibility that trafficking steps other than endocytosis, for example, recycling, are affected by the MSD mutations analyzed. It has proven technically difficult to approximate the wild-type Env recycling rate; slow Env endocytosis (10% in 10 min) provides a pool of labeled, internal Env proteins too small for accurate monitoring of Env reappearance on the cell surface (low signal-to-noise ratio). We are, however, confident that potential differences in recycling did not hamper measurement of endocytosis rates during the first 10 min of a chase at 37°C (33).

Mutations in the transmembranal domains of Env-μ26 (L165R; introduce charge) and Env-palm#7 and Env-palm#6 (C167C and C164G; lead to monoacylation) are likely to induce conformational changes. Such changes might be "translated" into altered recognition of the tyrosine motif in the cytoplasmic tail, thereby activating the "dormant" internalization motif to various extents, resulting in increased uptake rates of 4.7 and 7.4%/min for Env-S19-palm#7 and Env-S19-μ26, respectively. While we cannot distinguish if Env-S19-palm#6 (1.3%/min) was internalized with a rate above that of bulk uptake, the significantly faster internalization of the two other transmembranal mutants ($P \leq 0.005$; one-sided t test) is consistent with this interpretation. This demonstrates that the palmitoylation status per se does not determine uptake rates. It is noteworthy that the efficiently internalized HIV and SIV TM proteins naturally contain a charged residue in the designated transmembranal domain. Biochemical and electron microscopic evidence corroborates that these lentiviral Env proteins

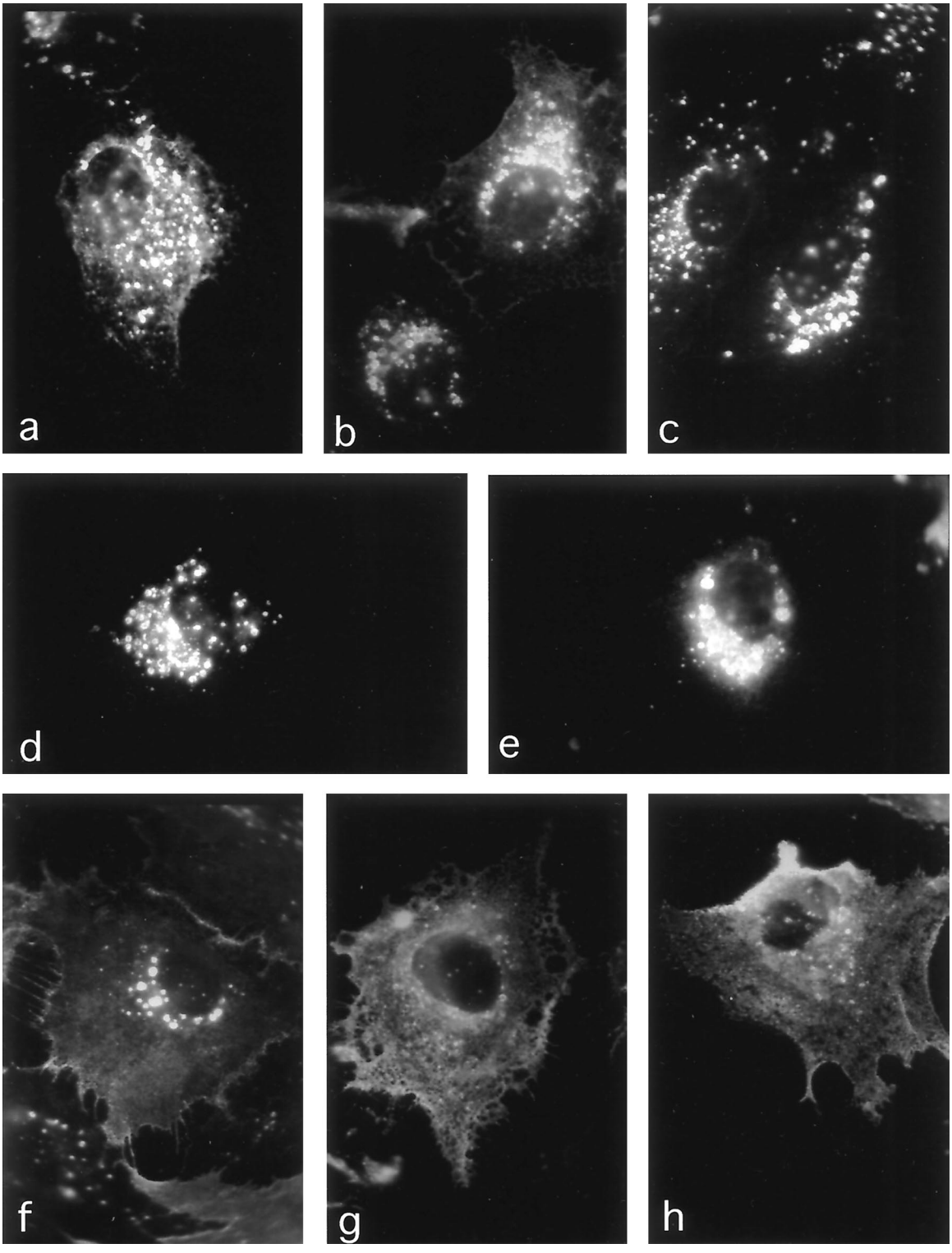

FIG. 6. Uptake of surface-bound neutralizing anti-Env antibody as demonstrated by indirect immunofluorescence confirms endocytosis phenotypes of MSD and cytoplasmic tail mutants. Triplicates of CV-1 cells grown on glass coverslips were infected with wild-type or mutant Env-S19-expressing SV40 lysates. At 2 days postinfection one set of coverslips was incubated with neutralizing chicken anti-RSV PrC serum in DMEM–100 μM chloroquine at 37°C for 2 h to allow for antibody internalization. Then, cells were fixed in methanol-acetic acid, stained with rb anti-chicken-FITC, and observed with a fluorescence microscope (Zeiss) as described in Materials and Methods. One set was fixed in acetone and prepared for whole-cell anti-Env immunofluorescence (not shown). The third set was incubated with rb#2 anti-Env serum on ice, fixed, and prepared for surface immunofluorescence (not shown). (a) Env-S19 wild type; (b) Env-S19-μ26; (c) Env-S19-palm#6; (d and e) Env-S19-palm#7; (f and g) Env-S19-Y190A; (h) Env-S19-N185*. Brightly stained vesicles represent endocytic prelysosomal vesicles, most likely late endosomes (27) (chloroquine inhibits fusion with lysosomes and lysosomal degradation). The net-like pattern observed for Env-S19-Y190A and Env-S19-N185* represents antibody bound to surface-expressed Env.

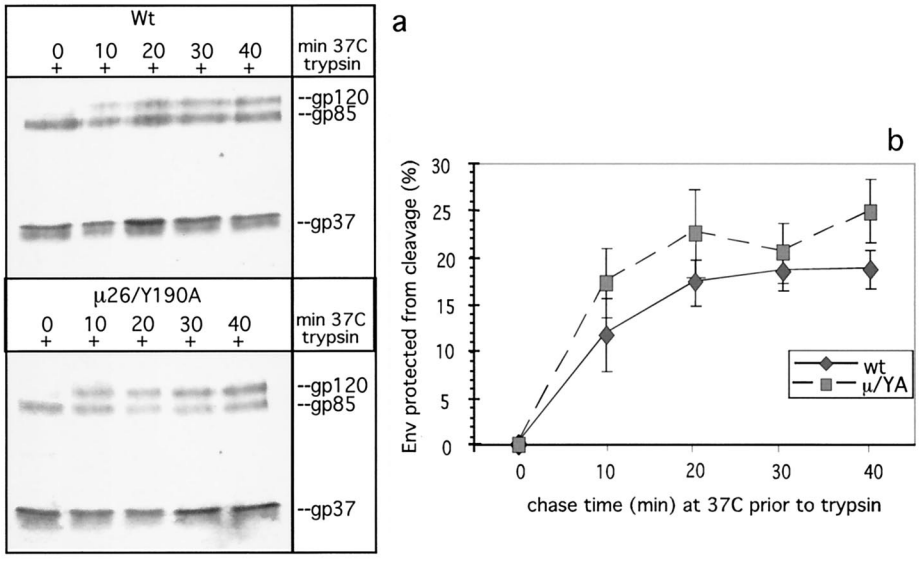

FIG. 7. In Env-S19-μ26/Y190A, the MSD (μ26 = L165R) and cytoplasmic tail (Y190A) mutations partly compensate one another's phenotype. The kinetics of internalization of Env-S19 and Env-S19-μ26/Y190A were analyzed essentially as described before. (a) Autoradiogram of a representative experiment. Wt, wild type. (b) Average kinetic data from four independent experiments, including error bars. Average internalization after the initial 10 min of the biphasic curves was 11.7% for wild-type (wt) Env-S19 and 17.2% for Env-S19-μ26/Y190A (μ/YA).

are clustered into clathrin-coated pits and are efficiently endocytosed by virtue of their tyrosine motifs (4, 42). The internalization phenotype of the RSV Env-S19-μ26/Y190A double mutant mirrors that observed upon mutation of crucial tyrosines in the SIV (Y_{723}) or HIV-1 (Y_{712}) TM cytoplasmic domains and deletion of the VZV gE cytoplasmic tail (4, 44, 56, 57). In all cases endocytosis is reduced to approximately the bulk uptake rate. The Env-S19-μ26/Y190A mutant also confirms that Y_{190} in the RSV TM is crucially involved in the μ26 rapid-uptake phenotype.

Bulk uptake does not require any specific signals since no active clustering occurs and proteins are carried passively into coated pits for endocytosis (63). Why then does the mutation of Y_{190} to alanine result in Env internalization significantly slower than that of the wild type and similar to that of influenza virus HA (which does not possess a YXXØ motif)? Mutations that disrupt sequences important for efficient endocytosis of cellular receptors, such as TfR or CD4, result in internalization rates above or equal to bulk membrane turnover (24, 25, 50), which is analogous to the situation for lentiviral Env proteins. The vesicular stomatitis virus (VSV) G protein resembles RSV Env inasmuch as it is endocytosed at approximately the bulk rate despite the presence of a tyrosine-based motif (21, 61). However, this YXXØ motif is crucial for basolateral targeting, not endocytosis, and mutation of the VSV G tyrosine motif did not result in a further drop of the internalization rate (61, 62). In contrast, preliminary observations in our laboratory do not suggest a crucial role of Y_{190} in basolateral targeting of the RSV glycoprotein. Thus, the results obtained from each of these systems is distinct from those from the endocytosis phenotypes we have observed for RSV. To our knowledge this is the first report of a system where substitution of the tyrosine within a YXXØ endocytosis motif results in a reduction of the internalization rate below that of bulk flow.

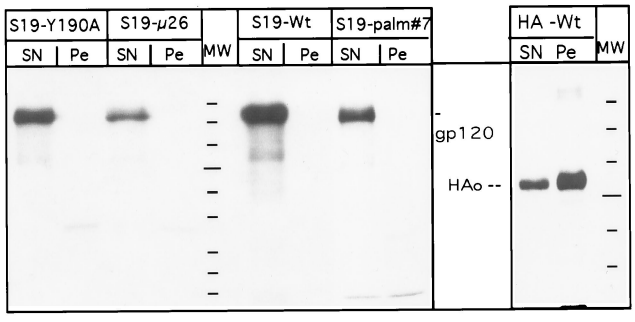

FIG. 8. Env-S19 MSD and cytoplasmic tail mutants show no difference with respect to DIG association. CV-1 cells infected with SV40 lysates expressing the indicated Env-S19 mutants or wild-type (wt) influenza virus HA_{Jap} were metabolically labeled and chased for 2 h as described in Materials and Methods. After surface biotinylation on ice, cells were lysed on ice for 6 min in buffer containing 1% Triton X-100 as specified in Materials and Methods. Lysates were spun at 12,000 × *g* for 6 min to separate solubilized material (SN) from the pellet (Pe) containing nuclei and membrane fractions insoluble under the chosen detergent and temperature conditions (DIGs or rafts [58]). Supernatants were adjusted to an SDS concentration of 0.1%, and pellets were lysed in 1% Triton X-100–1% DOC–0.1% SDS. Env and HA proteins, either solubilized or associated with DIGs, were recovered by immunoprecipitation followed by streptavidin-agarose bead precipitation. Three-fourths of each sample was analyzed by SDS-PAGE and autoradiography. HAo, uncleaved HA.

Other situations in which glycoproteins are efficiently excluded from endocytosis have been described. For example, CD4 containing an intact, or mutated, endocytosis motif is actively excluded from endocytic structures through interaction of its cytoplasmic domain with $p56^{lck}$. In the absence of $p56^{lck}$, wild-type CD4 is clustered into vesicles with an uptake rate of about 2 to 4%/min (47–49), while YXXØ motif mutants internalize at the bulk rate. Thus, interaction with a cytoplasmic binding partner can result in coated-pit exclusion. In contrast, wild-type HA, which internalizes at a rate of approximately 0.2%/min in CV-1 cells (32), was found to be actively excluded from coated pits (6, 33, 55) by virtue of sequences within its MSD (32). Mutants with certain changes in that part of the MSD in contact with the outer lipid leaflet were no longer excluded (32). Some, but not all, of these HA MSD mutants also showed a loss of HA's efficient association with

DIGs (58). Thus, for HA, there might exist some correlation between protein sequestering into certain plasma membrane domains and exclusion from clathrin vesicles. In this case, however, functional YXXØ motifs introduced into the cytoplasmic domain of HA appear to act dominantly over the MSD retention signals since rapid endocytosis now takes place (30, 32, 33, 35). We, therefore, examined whether the different RSV Env MSD and C-terminal tail mutants might display a differential pattern of DIG association (i.e., strong association for Env-S19-Y190A, low or no association for Env-S19-μ26 and Env-S19-palm#7, respectively), which could control the extent to which the proteins are excluded from clathrin-coated pits, particularly since Melkonian et al. (40) had shown that the extent of palmitoylation can modulate association with DIGs. We found no evidence that any of the Env proteins partitioned into DIGs. Nevertheless, this does not rule out the possibility that the wild-type and mutant Env proteins are associated with different membrane microdomains, not identified by the assays employed here, that define accessibility and recruitment into coated pits.

These results suggested that activity of the RSV Env endocytosis motif might be induced by conformational changes due to receptor binding or due to mutations in the transmembranal domain (as in Env-μ26 and Env-palm#7). Removal of Env from the cell surface upon interaction with its cognate receptor, expressed either on the same or on a neighboring cell, could have important biological implications. The binding of a neutralizing chicken antibody to cell surface-exposed Env, however, did not result in any significant enhancement of RSV Env-S19 endocytosis, which is in accordance with the results of similar approaches by others (57, 59). To directly test the receptor-binding activation hypothesis, it will be necessary to engineer the S19 and tyrosine motif mutations into an A subgroup virus for which the receptor gene has been cloned (3, 66); to date the cognate receptor for the PrC strain of RSV has not been identified.

Two different models can be proposed to account for the phenotypes of mutant RSV Env proteins. In one model, the transmembranal domain of the RSV TM would harbor information that causes the protein to be efficiently excluded from coated pits, either by differential association with membrane subdomains or by a conformational incompatibility with clustering. On the other side, the YXXØ endocytosis motif contained in the cytoplasmic tail would preferentially direct the Env protein to sites of active recruitment into endocytic vesicles. In this situation, sequences in the MSD would thus have a silencing effect on an active internalization signal, resulting in an internalization rate reminiscent of that of bulk uptake, but not in fact mediated by a "bulk" membrane turnover mechanism. In a biological context, such silencing might be overcome by activation events (such as receptor binding) that either remove the exclusion signal through conformational changes or enhance the efficiency with which the Y motif can be recognized by AP-2. The phenotypes observed for μ26, palm#7 and, to a lesser extent, palm#6 can be considered evidence for the first interpretation. The very low internalization rate of Env-S19-Y190A (0.3%/min) is consistent with the idea that the MSD harbors an "exclusion signal" that becomes dominant in the absence of Y_{190}. Env-S19-μ26/Y190A would then undergo true bulk uptake since both counteracting signals are lost in this mutant.

In a second, and less attractive, model, no exclusion signal would exist in the MSD. Instead, the YXXØ motif in the cytoplasmic tail would be constitutively inactive, resulting in genuine bulk uptake of wild-type Env. The MSD mutants we analyzed might simply induce conformational changes that enhance the recognition of the otherwise dormant endocytosis signal. Interestingly, the RSV TM mutant Env-S19-μ26 (L165R) resembles the HIV and SIV TM proteins inasmuch as their MSDs include a charged amino acid and the lentiviral Env proteins are constitutively internalized at a high rate. The significant drop in internalization observed for Env-S19-Y190A, on the other hand, might result from changes in the cytoplasmic tail that now prevent the Env trimer from participating in even bulk uptake. This could reflect an interaction with a cellular factor, such as that seen with CD4 and $p56^{lck}$. However, such a model would not readily explain the bulk rate endocytosis phenotype observed for the Env-S19-μ26/Y190A double mutant.

Additional experiments in progress are aimed at further defining the molecular mechanisms underlying the phenotypes we have observed. It will be important to clarify if endocytosis of RSV Env is in fact activatable and to examine the effects of alterations in the rate at which Env is internalized on the infectivity in vitro and pathogenesis in vivo of mutant ALSVs.

ACKNOWLEDGMENTS

We thank Jim Collawn (University of Alabama at Birmingham [UAB]) and Thomas Wilk and Peter Scheiffele (EMBL, Heidelberg, Germany) for stimulating discussion. We are grateful to Jim Collawn and Mike Sakalian (UAB) for critically reading the manuscript.

This work was supported by grant R37CA29884-16 from the National Institutes of Health. C.O. received a research fellowship from the Deutsche Forschungsgemeinschaft.

REFERENCES

1. **Ball, J. M., M. J. Mulligan, and R. W. Compans.** 1997. Basolateral sorting of the HIV type 2 and SIV envelope glycoproteins in polarized epithelial cells: role of the cytoplasmic domain. AIDS Res. Hum. Retrovir. **13:**665–675.
2. **Bansal, A., and L. M. Gierasch.** 1991. The NPXY internalization signal of the LDL receptor adopts a reverse-turn conformation. Cell **67:**1195–1201.
3. **Bates, P., J. A. Young, and H. E. Varmus.** 1993. A receptor for subgroup A Rous sarcoma virus is related to the low density lipoprotein receptor. Cell **74:**1043–1051.
4. **Boge, M., S. Wyss, J. S. Bonifacino, and M. Thali.** 1998. A membrane-proximal tyrosine-based signal mediates internalization of the HIV-1 envelope glycoprotein via interaction with the AP-2 clathrin adaptor. J. Biol. Chem. **273:**15773–15778.
5. **Boll, W., H. Ohno, Z. Songyang, I. Rapoport, L. C. Cantley, J. S. Bonifacino, and T. Kirchhausen.** 1996. Sequence requirements for the recognition of tyrosine-based endocytic signals by clathrin AP-2 complexes. EMBO J. **15:** 5789–5795.
6. **Bretscher, M. S., J. N. Thomson, and B. M. Pearse.** 1980. Coated pits act as molecular filters. Proc. Natl. Acad. Sci. USA **77:**46–49.
7. **Brewer, C. B., and M. G. Roth.** 1991. A single amino acid change in the cytoplasmic domain alters the polarized delivery of influenza virus hemagglutinin. J. Cell Biol. **114:**413–421.
8. **Brown, M. S., R. G. Anderson, and J. L. Goldstein.** 1983. Recycling receptors: the round-trip itinerary of migrant membrane proteins. Cell **32:**663–667.
9. **Chang, C. P., C. S. Lazar, B. J. Walsh, M. Komuro, J. F. Collawn, L. A. Kuhn, J. A. Tainer, I. S. Trowbridge, M. G. Farquhar, M. G. Rosenfeld, et al.** 1993. Ligand-induced internalization of the epidermal growth factor receptor is mediated by multiple endocytic codes analogous to the tyrosine motif found in constitutively internalized receptors. J. Biol. Chem. **268:** 19312–19320.
10. **Chen, W. S., C. S. Lazar, K. A. Lund, J. B. Welsh, C. P. Chang, G. M. Walton, C. J. Der, H. S. Wiley, G. N. Gill, and M. G. Rosenfeld.** 1989. Functional independence of the epidermal growth factor receptor from a domain required for ligand-induced internalization and calcium regulation. Cell **59:**33–43.
11. **Collawn, J. F., L. A. Kuhn, L. F. Liu, J. A. Tainer, and I. S. Trowbridge.** 1991. Transplanted LDL and mannose-6-phosphate receptor internalization signals promote high-efficiency endocytosis of the transferrin receptor. EMBO J. **10:**3247–3253.
12. **Collawn, J. F., M. Stangel, L. A. Kuhn, V. Esekogwu, S. Q. Jing, I. S. Trowbridge, and J. A. Tainer.** 1990. Transferrin receptor internalization sequence YXRF implicates a tight turn as the structural recognition motif for endocytosis. Cell **63:**1061–1072.
13. **Davis, G. L., and E. Hunter.** 1987. A charged amino acid substitution within the transmembrane anchor of the Rous sarcoma virus envelope glycoprotein

affects surface expression but not intracellular transport. J. Cell Biol. **105:** 1191–1203.
14. **Dong, J., M. G. Roth, and E. Hunter.** 1992. A chimeric avian retrovirus containing the influenza virus hemagglutinin gene has an expanded host range. J. Virol. **66:**7374–7382.
15. **Dong, J. Y., J. W. Dubay, L. G. Perez, and E. Hunter.** 1992. Mutations within the proteolytic cleavage site of the Rous sarcoma virus glycoprotein define a requirement for dibasic residues for intracellular cleavage. J. Virol. **66:**865–874.
16. **Dubay, J. W., S. J. Roberts, B. H. Hahn, and E. Hunter.** 1992. Truncation of the human immunodeficiency virus type 1 transmembrane glycoprotein cytoplasmic domain blocks virus infectivity. J. Virol. **66:**6616–6625.
17. **Eberle, W., C. Sander, W. Klaus, B. Schmidt, K. von Figura, and C. Peters.** 1991. The essential tyrosine of the internalization signal in lysosomal acid phosphatase is part of a beta turn. Cell **67:**1203–1209.
18. **Egan, M. A., L. M. Carruth, J. F. Rowell, X. Yu, and R. F. Siliciano.** 1996. Human immunodeficiency virus type 1 envelope protein endocytosis mediated by a highly conserved intrinsic internalization signal in the cytoplasmic domain of gp41 is suppressed in the presence of the $Pr55^{gag}$ precursor protein. J. Virol. **70:**6547–6556.
19. **Geffen, I., C. Fuhrer, B. Leitinger, M. Weiss, K. Huggel, G. Griffiths, and M. Spiess.** 1993. Related signals for endocytosis and basolateral sorting of the asialoglycoprotein receptor. J. Biol. Chem. **268:**20772–20777.
20. **Ghosh, R. N., W. G. Mallet, T. T. Soe, T. E. McGraw, and F. R. Maxfield.** 1998. An endocytosed TGN38 chimeric protein is delivered to the TGN after trafficking through the endocytic recycling compartment in CHO cells. J. Cell Biol. **142:**923–936.
21. **Gottlieb, T. A., I. E. Ivanov, M. Adesnik, and D. D. Sabatini.** 1993. Actin microfilaments play a critical role in endocytosis at the apical but not the basolateral surface of polarized epithelial cells. J. Cell Biol. **120:**695–710.
22. **Griffiths, G., R. Back, and M. Marsh.** 1989. A quantitative analysis of the endocytic pathway in baby hamster kidney cells. J. Cell Biol. **109:**2703–2720.
23. **Hunziker, W., and C. Fumey.** 1994. A di-leucine motif mediates endocytosis and basolateral sorting of macrophage IgG Fc receptors in MDCK cells. EMBO J. **13:**2963–2967.
24. **Jing, S., and I. Trowbridge.** 1990. Nonacylated human transferrin receptors are rapidly internalized and mediate iron uptake. J. Biol. Chem. **265:**11555–11559.
25. **Jing, S. Q., T. Spencer, K. Miller, C. Hopkins, and I. S. Trowbridge.** 1990. Role of the human transferrin receptor cytoplasmic domain in endocytosis: localization of a specific signal sequence for internalization. J. Cell Biol. **110:**283–294.
26. **Johnson, L. S., K. W. Dunn, B. Pytowski, and T. E. McGraw.** 1993. Endosome acidification and receptor trafficking: bafilomycin A1 slows receptor externalization by a mechanism involving the receptor's internalization motif. Mol. Biol. Cell **4:**1251–1266.
27. **Johnston, P. B., J. Y. Dong, and E. Hunter.** 1995. Transport of a lysosomally targeted Rous sarcoma virus envelope glycoprotein involves transient expression on the cell surface. Virology **206:**353–361.
28. **Kang, S., L. Liang, C. D. Parker, and J. F. Collawn.** 1998. Structural requirements for major histocompatibility complex class II invariant chain endocytosis and lysosomal targeting. J. Biol. Chem. **273:**20644–20652.
29. **Katz, R. A., C. A. Omer, J. H. Weis, S. A. Mitsialis, A. J. Faras, and R. V. Guntaka.** 1982. Restriction endonuclease and nucleotide sequence analysis of molecularly cloned unintegrated avian tumor virus DNA: structure of large terminal repeats in circular junctions. J. Virol. **42:**346–351.
30. **Ktistakis, N. T., D. Thomas, and M. G. Roth.** 1990. Characteristics of the tyrosine recognition signal for internalization of transmembrane surface glycoproteins. J. Cell Biol. **111:**1393–1407.
31. **LaBranche, C. C., M. M. Sauter, B. S. Haggarty, P. J. Vance, J. Romano, T. K. Hart, P. J. Bugelski, M. Marsh, and J. A. Hoxie.** 1995. A single amino acid change in the cytoplasmic domain of the simian immunodeficiency virus transmembrane molecule increases envelope glycoprotein expression on infected cells. J. Virol. **69:**5217–5227.
32. **Lazarovits, J., H. Y. Naim, A. C. Rodriguez, R. H. Wang, E. Fire, C. Bird, Y. I. Henis, and M. G. Roth.** 1996. Endocytosis of chimeric influenza virus hemagglutinin proteins that lack a cytoplasmic recognition feature for coated pits. J. Cell Biol. **134:**339–348.
33. **Lazarovits, J., and M. Roth.** 1988. A single amino acid change in the cytoplasmic domain allows the influenza virus hemagglutinin to be endocytosed through coated pits. Cell **53:**743–752.
34. **Lazarovits, J., S. P. Shia, N. Ktistakis, M. S. Lee, C. Bird, and M. G. Roth.** 1990. The effects of foreign transmembrane domains on the biosynthesis of the influenza virus hemagglutinin. J. Biol. Chem. **265:**4760–4767.
35. **Lin, S., H. Y. Naim, and M. G. Roth.** 1997. Tyrosine-dependent basolateral sorting signals are distinct from tyrosine-dependent internalization signals. J. Biol. Chem. **272:**26300–26305.
36. **Lippincott-Schwartz, J., and D. M. Fambrough.** 1987. Cycling of the integral membrane glycoprotein, LEP100, between plasma membrane and lysosomes: kinetic and morphological analysis. Cell **49:**669–677.
37. **Lodge, R., H. Göttlinger, D. Gabuzda, E. A. Cohen, and G. Lemay.** 1994. The intracytoplasmic domain of gp41 mediates polarized budding of human immunodeficiency virus type 1 in MDCK cells. J. Virol. **68:**4857–4861.
38. **Lodge, R., J. P. Lalonde, G. Lemay, and E. A. Cohen.** 1997. The membrane-proximal intracytoplasmic tyrosine residue of HIV-1 envelope glycoprotein is critical for basolateral targeting of viral budding in MDCK cells. EMBO J. **16:**695–705.
39. **Mayor, S., J. F. Presley, and F. R. Maxfield.** 1993. Sorting of membrane components from endosomes and subsequent recycling to the cell surface occurs by a bulk flow process. J. Cell Biol. **121:**1257–1269.
40. **Melkonian, K. A., A. G. Ostermeyer, J. Z. Chen, M. G. Roth, and D. A. Brown.** 1999. Role of lipid modifications in targeting proteins to detergent-resistant membrane rafts. Many raft proteins are acylated, while few are prenylated. J. Biol. Chem. **274:**3910–3917.
41. **Mukherjee, S., R. N. Ghosh, and F. R. Maxfield.** 1997. Endocytosis. Physiol. Rev. **77:**759–803.
42. **Ohno, H., R. C. Aguilar, M. C. Fournier, S. Hennecke, P. Cosson, and J. S. Bonifacino.** 1997. Interaction of endocytic signals from the HIV-1 envelope glycoprotein complex with members of the adaptor medium chain family. Virology **238:**305–315.
43. **Ohno, H., J. Stewart, M. C. Fournier, H. Bosshart, I. Rhee, S. Miyatake, T. Saito, A. Gallusser, T. Kirchhausen, and J. S. Bonifacino.** 1995. Interaction of tyrosine-based sorting signals with clathrin-associated proteins. Science **269:**1872–1875.
44. **Olson, J. K., and C. Grose.** 1997. Endocytosis and recycling of varicella-zoster virus Fc receptor glycoprotein gE: internalization mediated by a YXXL motif in the cytoplasmic tail. J. Virol. **71:**4042–4054.
45. **Owens, R. J., and R. W. Compans.** 1989. Expression of the human immunodeficiency virus envelope glycoprotein is restricted to basolateral surfaces of polarized epithelial cells. J. Virol. **63:**978–982.
46. **Owens, R. J., J. W. Dubay, E. Hunter, and R. W. Compans.** 1991. Human immunodeficiency virus envelope protein determines the site of virus release in polarized epithelial cells. Proc. Natl. Acad. Sci. USA **88:**3987–3991.
47. **Pelchen-Matthews, A., J. E. Armes, G. Griffiths, and M. Marsh.** 1991. Differential endocytosis of CD4 in lymphocytic and nonlymphocytic cells. J. Exp. Med. **173:**575–587.
48. **Pelchen-Matthews, A., I. Boulet, D. R. Littman, R. Fagard, and M. Marsh.** 1992. The protein tyrosine kinase $p56^{lck}$ inhibits CD4 endocytosis by preventing entry of CD4 into coated pits. J. Cell Biol. **117:**279–290.
49. **Pelchen-Matthews, A., P. Clapham, and M. Marsh.** 1995. Role of CD4 endocytosis in human immunodeficiency virus infection. J. Virol. **69:**8164–8168.
50. **Pelchen-Matthews, A., I. J. Parsons, and M. Marsh.** 1993. Phorbol ester-induced downregulation of CD4 is a multistep process involving dissociation from $p56^{lck}$, increased association with clathrin-coated pits, and altered endosomal sorting. J. Exp. Med. **178:**1209–1222.
51. **Pipas, J. M., K. W. C. Peden, and D. Nathans.** 1983. Mutational analysis of simian virus 40 T antigen: isolation and characterization of mutants with deletions in the T-antigen gene. Mol. Cell. Biol. **3:**203–213.
52. **Pytowski, B., T. W. Judge, and T. E. McGraw.** 1995. An internalization motif is created in the cytoplasmic domain of the transferrin receptor by substitution of a tyrosine at the first position of a predicted tight turn. J. Biol. Chem. **270:**9067–9073.
53. **Reaves, B. J., G. Banting, and J. P. Luzio.** 1998. Lumenal and transmembrane domains play a role in sorting type I membrane proteins on endocytic pathways. Mol. Biol. Cell **9:**1107–1122.
54. **Rohrer, J., A. Schweizer, D. Russell, and S. Kornfeld.** 1996. The targeting of Lamp1 to lysosomes is dependent on the spacing of its cytoplasmic tail tyrosine sorting motif relative to the membrane. J. Cell Biol. **132:**565–576.
55. **Roth, M. G., C. Doyle, J. Sambrook, and M. J. Gething.** 1986. Heterologous transmembrane and cytoplasmic domains direct functional chimeric influenza virus hemagglutinins into the endocytic pathway. J. Cell Biol. **102:**1271–1283.
56. **Rowell, J. F., P. E. Stanhope, and R. F. Siliciano.** 1995. Endocytosis of endogenously synthesized HIV-1 envelope protein. J. Immunol. **155:**473–488.
57. **Sauter, M. M., A. Pelchen-Matthews, R. Bron, M. Marsh, C. C. LaBranche, P. J. Vance, J. Romano, B. S. Haggarty, T. K. Hart, W. M. Lee, and J. A. Hoxie.** 1996. An internalization signal in the simian immunodeficiency virus transmembrane protein cytoplasmic domain modulates expression of envelope glycoproteins on the cell surface. J. Cell Biol. **132:**795–811.
58. **Scheiffele, P., M. G. Roth, and K. Simons.** 1997. Interaction of influenza virus haemagglutinin with sphingolipid-cholesterol membrane domains via its transmembrane domain. EMBO J. **16:**5501–5508.
59. **Signoret, N., J. Oldridge, A. Pelchen-Matthews, P. J. Klasse, T. Tran, L. F. Brass, M. M. Rosenkilde, T. W. Schwartz, W. Holmes, W. Dallas, M. A. Luther, T. N. Wells, J. A. Hoxie, and M. Marsh.** 1997. Phorbol esters and SDF-1 induce rapid endocytosis and down modulation of the chemokine receptor CXCR4. J. Cell Biol. **139:**651–664.
60. **Stephens, D. J., and G. Banting.** 1998. Specificity of interaction between adaptor-complex medium chains and the tyrosine-based sorting motifs of TGN38 and lgp120. Biochem. J. **335:**567–572.
61. **Thomas, D. C., C. B. Brewer, and M. G. Roth.** 1993. Vesicular stomatitis virus glycoprotein contains a dominant cytoplasmic basolateral sorting signal

critically dependent upon a tyrosine. J. Biol. Chem. **268:**3313–3320.
62. **Thomas, D. C., and M. G. Roth.** 1994. The basolateral targeting signal in the cytoplasmic domain of glycoprotein G from vesicular stomatitis virus resembles a variety of intracellular targeting motifs related by primary sequence but having diverse targeting activities. J. Biol. Chem. **269:**15732–15739.
63. **Trowbridge, I. S., J. F. Collawn, and C. R. Hopkins.** 1993. Signal-dependent membrane protein trafficking in the endocytic pathway. Annu. Rev. Cell Biol. **9:**129–161.
64. **Watts, C., and M. Marsh.** 1992. Endocytosis: what goes in and how? J. Cell Sci. **103:**1–8.
65. **White, S., S. R. Hatton, M. A. Siddiqui, C. D. Parker, I. S. Trowbridge, and J. F. Collawn.** 1998. Analysis of the structural requirements for lysosomal membrane targeting using transferrin receptor chimeras. J. Biol. Chem. **273:**14355–14362.
66. **Young, J. A., P. Bates, and H. E. Varmus.** 1993. Isolation of a chicken gene that confers susceptibility to infection by subgroup A avian leukosis and sarcoma viruses. J. Virol. **67:**1811–1816.